ADVANCED MATERIALS
www.advmat.de

# Implementing Quantum Search Algorithm with Metamaterials

*Weixuan Zhang, Kaiyang Cheng, Chao Wu, Yi Wang, Hongqiang Li,* and Xiangdong Zhang**

**Metamaterials, artificially structured electromagnetic (EM) materials, have enabled the realization of many unconventional EM properties not found in nature, such as negative refractive index, magnetic response, invisibility cloaking, and so on. Based on these man-made materials with novel EM properties, various devices are designed and realized. However, quantum analog devices based on metamaterials have not been achieved so far. Here, metamaterials are designed and printed to perform quantum search algorithm. The structures, comprising of an array of 2D subwavelength air holes with different radii perforated on the dielectric layer, are fabricated using a 3D-printing technique. When an incident wave enters in the designed metamaterials, the profile of beam wavefront is processed iteratively as it propagates through the metamaterial periodically. After $\approx \sqrt{N}$ roundtrips, precisely the same as the efficiency of quantum search algorithm, searched items will be found with the incident wave all focusing on the marked positions. Such a metamaterial-based quantum searching simulator may lead to remarkable achievements in wave-based signal processors.**

In recent years, many efforts have been devoted to the design and realization of metamaterials since the experimental demonstration of negative refraction in 2001.[1] After nearly 20 years of research, different types of metamaterials from microwave to visible frequencies have been fabricated, such as negative index metamaterials,[1–6] artificial magnetism metamaterials,[7,8] transformation optics metamaterials,[9–11] hyperbolic metamaterials,[12,13] active metamaterials,[14–16] nonlinear metamaterials,[17] quantum metamaterials,[18–20] and so on.[21–27] Recently, the concept of "computational metamaterials" has been proposed.[28–33] Mathematical operations, such as spatial differentiation, integration, and convolution, can be performed by using designed metamaterial blocks. The dimension at wavelength scale of such kind of computing machines offers the possibility of miniaturized full-wave computing systems that are several orders of magnitude thinner than conventional bulky lens-based optical processors.

On the other hand, quantum computation has been the focus of numerous studies and is expected to play an important role in future information processing since it outperforms classical computation at many tasks.[34] The excitement over quantum computation is based on just a few algorithms, the best known being Shor's factorization algorithm[35] and Grover's search algorithm.[36] The latter is extremely important, both from a fundamental standpoint, as it is usually more efficient than the best classical algorithm, and from a practical standpoint, because fast searching is central to solving difficult problems. Up to now, Grover's search algorithm has been implemented under many standard circuit models, such as optical experiments,[37,38] NMR systems,[39,40] trapped ion,[41] and so on. The problem is whether Grover's search algorithm can be performed by using designed metamaterials. In this work, we numerically and experimentally demonstrate the implementation of Grover's search algorithm through dielectric metamaterials at microwave frequencies.

The general protocol is graphically shown in **Figure 1**a with different colors being used to distinguish the structural regions that perform different functions. In this metamaterial-based searching protocol, the electric field amplitude of the incident microwave "$E(y)$" is recognized as the probability amplitude of the equivalent quantum state, spatial positions "$y$" are used to label the items in the database, and the maximum number of the database is fixed by the full width at half-maximum (FWHM) "$D$" of the incident intensity profile with near-Gaussian distribution. The designed metamaterial is comprised of four cascaded subblocks: an oracle subblock (red area, $U_m$), two Fourier transform subblocks (green areas, $F$), and a phase plate subblock (blue area, $U_0$). The role of the oracle subblock is to mark the targeted item (red arrow) $|y = m\rangle$

Dr. W. Zhang, Prof. X. Zhang
Beijing Key Laboratory of Nanophotonics and Ultrafine Optoelectronic Systems
School of Physics
Beijing Institute of Technology
100081 Beijing, China
E-mail: zhangxd@bit.edu.cn
Dr. K. Cheng, Dr. C. Wu, Dr. Y. Wang, Prof. H. Li
The Institute of Dongguan-Tongji University
Dongguan, Guangdong 523808, China
E-mail: hqlee@tongji.edu.cn
Dr. K. Cheng, Dr. C. Wu, Dr. Y. Wang, Prof. H. Li
School of Physics Science and Engineering
Tongji University
Shanghai 200092, China
The ORCID identification number(s) for the author(s) of this article can be found under https://doi.org/10.1002/adma.201703986.

**DOI: 10.1002/adma.201703986**

 

by imprinting a spatially dependent phase profile on the incident beam, $E(\gamma) - E(\gamma)\exp(i2\pi\sqrt{\varepsilon_{\mathrm{m}}(\gamma)}d_{\mathrm{m}}/\lambda_0)$, where $\lambda_0$ is the wavelength of the incident beam in vacuum, and $d_{\mathrm{m}}$ and $\varepsilon_{\mathrm{m}}(\gamma)$ are the length and effective permittivity of the subblock, respectively. Here, $0.5\pi$ phase transition is added in the narrow area around the tagged items and $0\pi$ phase transition elsewhere. A combination of two Fourier transform subblocks and the phase plate subblock can convert the phase difference marked by the oracle subblock into amplitude information by the sequences $\approx FU$

Figure 1b presents the photograph of the printed metamaterial (3 cm thick) with the corresponding parameters being $\varepsilon_c = 3.0$, $d_m = d_0 = 3a$, $W = 51a$ and $l = 57a$, respectively. Here, $a$ (≈0.4 cm) is the size of the unit cell that divides our metamaterial system into a series of small square grids. The designed GRIN block consists of 51 × 57 holes, and each hole occupies a 0.4 × 0.4 cm$^2$ square cell. The largest radius at the position of $y = \pm 10$ cm is 0.1904 cm, and the smallest radius at $y = 0.4$ cm is 0.0076 cm (0 cm at $y = 0$). In the case of the $U_{0(m)}$ block, it is composed of 51 × 3 holes, and each hole occupies the same square cell as the GRIN block. The radius at the position with $0.5\pi$ phase transition (from $-5a$ to $-3a$, blue arrow) is 0.1 cm, and the radius at the position with $0\pi$ phase transition is 0.1841 cm. In order to reduce the influence of the optical diffraction, the gradually varied radius (0.118, 0.134, 0.148, 0.161, and 0.173 cm) is used between the positions of the targeted items and surrounding areas. Moreover, the designed metamaterial can also perform multiitems search, when the oracle subblock possesses more than one marked positions. In this regard, we designed the second metamaterial with the tagged items lying at two different locations (blue arrows), as shown in Figure 1c. When the searching process is completed, the incident microwaves will focus on these two tagged positions.

In order to test the efficiency of the searching scheme, we perform full-wave numerical simulations using the finite-element method (COMSOL Multiphysics). **Figure 2**a shows the snapshot of the electric field intensity throughout the first metamaterial with the input function being $E(y) = \exp(-y^2/20)$. In this case, the FWHM value of the incident intensity equals $D = 5.26$ cm. In Figure 2b, we also plot the distribution of the wave intensity $|E(y)|^2$ at the output plane with 0.5-iteration. It is found that the incident wave is mainly focused on the position around the marked holes. However, there are still a few of the electric fields not concentrated on the searched positions. With the increase of the iterations, the concentration of electric fields will become more significant. This is equivalent to the condition that the probability of the searched state increases continuously (approaches to unity) with the increment of the searching time serially. Figure 2c presents the distribution of the output intensity with the beam propagating 1.5-roundtrips within the metamaterial. It is clearly shown that the output microwaves are nearly all concentrated on the marked positions with the corresponding FWHM being $d = 1.4$ cm. We need to emphasize that the FWHM value of the output intensity is not equal to the real size of the marked space due to the inhomogeneous distribution of the incident beam. Several little side peaks are result of the diffraction effect in the process of iterations. The corresponding snapshot of the field intensity is plotted in Figure 2d. The ratio $D/d$ can be interpreted as the size of the database ($N$) for a single item search. A straightforward calculation demonstrates that the number of iterations performed on the metamaterial is precisely consistent with the efficiency of the quantum search algorithm $\pi\sqrt{D/d}/4 \approx 1.5$ ,[36] when the marked items are located. It indicates that the designed metamaterial is capable of implementing the quantum search algorithm. The phenomenon originates from wave interference properties, entanglement is not necessary for the efficiency of quantum searching arithmetic, as noted in refs. [37,38].

The snapshot of the electric field intensity throughout the second metamaterial (with two marked items) is shown in Figure 2e. The output profile is presented in Figure 2f. We can see that only after 0.5-iteration, the incident electric fields

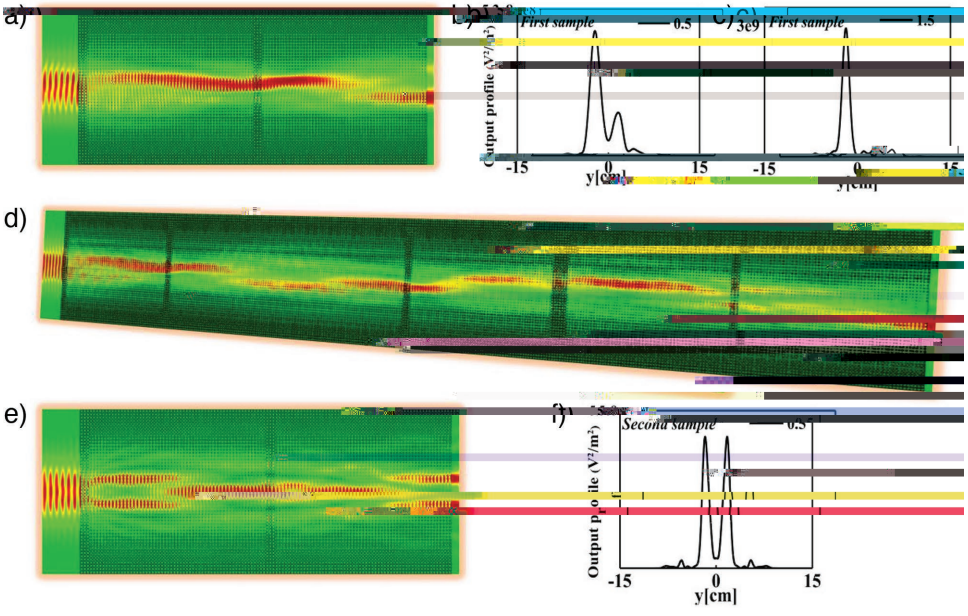


**Figure 2.** Theoretical simulation of the quantum search algorithm. a,d) The snapshots for the intensity of the incident microwave throughout the first metamaterial functioning as quantum searching simulator with 0.5- and 1.5-iterations, respectively. b,c) Simulation results for the output intensity of the first metamaterial with the incident wave propagating 0.5- and 1.5-roundtrips within the metamaterial, respectively. e) The snapshot for the intensity of the incident wave throughout the second metamaterial with 0.5-iteration. f) Simulation results for the output intensity of the second metamaterial with the incident wave propagating 0.5-roundtrip within the metamaterial.

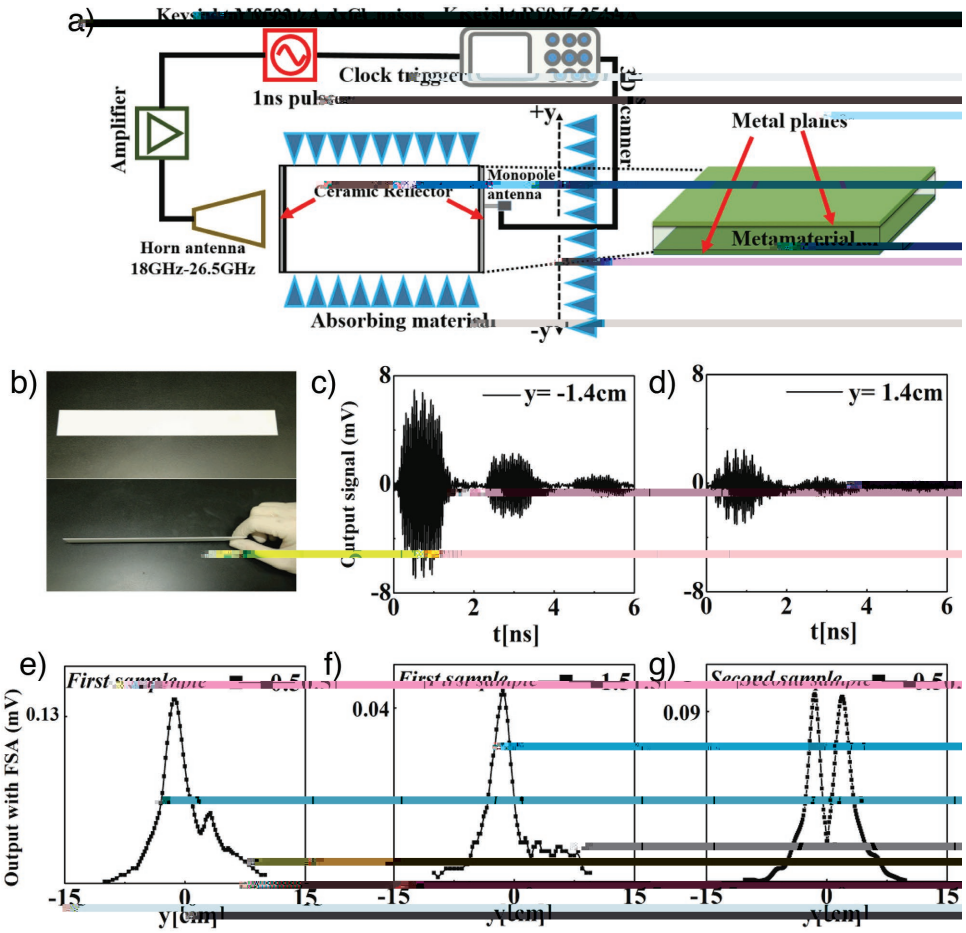


**Figure 3.** Experimental measurements of the quantum search algorithm. a) The conceptual drawing of the experimental setup. b) Photograph of the ceramic reflector. c,d) Time traces of the output intensities for the first metamaterial at positions of $y = -1.4$ cm and $y = 1.4$ cm, respectively. e,f) Experimental results for the profiles of the output intensity of the first metamaterial with 0.5- and 1.5-iterations, respectively. g) Experimental result for the profile of the output intensity of the second metamaterial with 0.5-iteration.

are nearly all concentrated on the two marked spaces. In fact, multiiterations searching processes (such as 2.0-iterations) can also be realized in such a case, which will exhibit $\approx \sqrt{N}$ scaling behaviors as expected from Grover's algorithm. The detailed results are provided in the Supporting Information.

To further validate our design, experimental measurements are carried out. The conceptual drawing of the experimental setup is illustrated in **Figure 3**a. In experiments, it is possible to reduce the microwave scattering to two dimensions by confining electromagnetic waves between two parallel conducting planes. The microwave cavity is surrounded by the absorbing materials to reduce the experimental errors induced by the optical scatterings. A beam with a near-Gaussian distribution in wavefront can be generated by a standard horn antenna at Ku band. The pulse signals, whose carrier frequency and period are 19.3 GHz and 100 ns, are generated by the arbitrary waveform generator (Keysight M9502A AxleChassis) with the pulse width, 1 ns, being short compared to the roundtrip time (about 2.87 ns), and so that the pulse signals belonging to different iterative times can be resolved by the oscilloscope (Keysight DS0-Z 254A) with the sampling frequency being 80 GHz. And a microwave amplifier (Keysight 83017A) is also used to ensure a big enough signal input for detection. In addition, in order to perform the searching process iteratively, we install two ceramic ($Al_2O_3$) sheets on both ends of the metamaterial to make the incident pulse travel back and forth within the cavity. Figure 3b presents the photograph of the ceramic sheet. The reflectivity of the ceramic sheet is about 55% with the corresponding thickness being 1 mm (see the Supporting Information). In Figures 3c,d, we plot two typical time traces with the probing pin (monopole antenna fixed on the 3D scanner) locating at $y = -1.4$ cm and $y = 1.4$ cm, respectively. Three discrete pulses in time domain, each with a width of about 1 ns, are clearly presented, which correspond to the searching signals for 0.5-, 1.5- and 2.5-iterations, respectively. The interval of the adjacent signals is both nearly 2.87 ns equaling to the time of the pulse travelling back and forth between the cavity mirrors. We can see that the intensities at $y = -1.4$ cm (marked position) are always larger than that at $y = 1.4$ cm. This is consistent with the fact that the incident microwaves are focused at the searched position and accumulated in time. We measured the entire beam profile by recording traces, just as in Figure 3c,d, at different positions. It is noted that the bandwidth of the 1 ns pulse signal is about 1 GHz. Consequently, the Fourier spectral

analysis (FSA) is needed to get the intensity of a specific frequency. Combining intensities on different positions, the transverse beam profile of the output signal can be drawn. The evolution of such profiles of different roundtrips shows how the algorithm proceeds.

As shown in Figure 3e,f, the experimental measured output profiles with 0.5- and 1.5-iterations are nearly consistent with the corresponding numerical simulations. The wider peak compared to the numerical solution is the result of the imperfect sample fabrication and minor variation for the incident wave profile compared to the ideal condition. For example, it is very difficult to print perfect air holes with small radii on the veroclear810 layer. On the other hand, the multiitems searching process with the other sample is also measured. As shown in Figure 3g, the incident microwaves are almost concentrated on the two marked positions with 0.5-iteration. The results of multiple tests are consistent. The experimental demonstration indicates that the quantum search algorithm can be simulated successfully using the designed metamaterials, both for cases with single and two marked items.

In summary, we have proposed and designed metamaterials to perform wave-based quantum search algorithm. To the best of our knowledge, no studies have dedicated on this topic before. Our numerical simulations and experiments clearly confirm that the searching efficiency, on such metamaterials fabricated by 3D-printing technology, is the same as quantum computing. Moreover, the general design principle in our device can be applied, in principle, to any wavelength. Apart from implementing Grover's search algorithm, other quantum algorithms can also be simulated based on the similar methods, such as Deutsch–Jozsa algorithm. Our metamaterial approach for an all-optical quantum searching simulator provides a new way to shed light on quantum analog behaviors, which may lead to remarkable achievements in wave-based signal processors.

## Experimental Section

3D printing was utilized for the rapid prototyping of 3D models originally generated by a computer-aided design program. The 3D printer (Objet 1000 plus) was controlled with the computer program (Objet studio) in this work. The printing temperature and humidity were 20 ° C and 54%, respectively. The temperature of the printing head was 67 °C. The support materials 249g sup705 and modeling materials 3578g veroclear810 were used. The printing time was 13.27 h. After the completion of the printing process, the support materials were needed to be clear away (water cannons flush tiny support materials) and the modeling materials were needed to be baked. The baking temperature and baking time were 50 °C and 10 h, respectively.

## Supporting Information

Supporting Information is available from the Wiley Online Library or from the author.

## Acknowledgements

W.Z. and K.C. contributed equally to this work. This work was supported by the National key R&D Program of China under Grant No. 2017YFA0303800 and the National Natural Science Foundation of China (Grant No. 11574031 and 61421001).

## Conflict of Interest

The authors declare no conflict of interest.

## Keywords

metamaterials, microwaves, quantum search algorithm

Received: July 17, 2017
Revised: September 28, 2017
Published online:

[1] R. A. Shelby, D. R. Smith, S. Schultz, *Science* **2001**, *292*, 77.
[2] V. G. Veselago, *Sov. Phys.-Usp.* **1968**, *10*, 509.
[3] J. B. Pendry, *Phys. Rev. Lett.* **2000**, *85*, 3966.
[4] N. Fang, H. Lee, C. Sun, X. Zhang, *Science* **2005**, *308*, 534.
[5] J. Valentine, S. Zhang, T. Zentgraf, E. Ulin-Avila, D. A. Genov, G. Bartal, X. Zhang, *Nature* **2008**, *455*, 376.
[6] N. Liu, H. Guo, L. Fu, S. Kaiser, H. Schweizer, H. Giessen, *Nat. Mater.* **2008**, *7*, 31.
[7] T. J. Yen, W. J. Padilla, N. Fang, D. C. Vier, D. R. Smith, J. B. Pendry, D. N. Basov, X. Zhang, *Science* **2004**, *303*, 1494.
[8] S. Linden, C. Enkrich, M. Wegener, J. F. Zhou, T. Koschny, C. M. Soukoulis, *Science* **2004**, *306*, 1351.
[9] J. B. Pendry, D. Schurig, D. R. Smith, *Science* **2006**, *312*, 1780.
[10] U. Leonhardt, *Science* **2006**, *312*, 1777.
[11] H. Chen, C. T. Chan, P. Sheng, *Nat. Mater.* **2010**, *9*, 387.
[12] A. Poddubny, I. Iorsh, P. Belov, Y. Kivshar, *Nat. Photonics* **2013**, *7*, 948.
[13] K. V. Sreekanth, Y. Alapan, M. Elkabbash, E. Llker, M. Hinczewski, U. A. Gurkan, A. D. Luca, G. Strangi, *Nat. Mater.* **2016**, *15*, 621.
[14] O. Hess, J. B. Pendry, S. A. Maier, R. F. Oulton, J. M. Hamm, K. L. Tsakmakidis, *Nat. Mater.* **2012**, *11*, 573.
[15] S. Xiao, V. P. Drachev, A. V. Kildishev, X. Ni, U. K. Chettiar, H. K. Yuan, V. M. Shalaev, *Nature* **2010**, *466*, 735.
[16] S. H. Lee, M. Choi, T. T. Kim, S. Lee, M. Liu, X. Yin, H. K. Choi, S. S. Lee, C. C. Choi, S. Y. Choi, X. Zhang, B. Min, *Nat. Mater.* **2012**, *11*, 936.
[17] M. W. Klein, C. Enkrich, M. Wegener, S. Linden, *Science* **2006**, *313*, 502.
[18] M. Ricci, N. Orloff, S. M. Anlage, *Appl. Phys. Lett.* **2005**, *87*, 034102.
[19] P. Macha, G. Oelsner, J. M. Reiner, M. Marthaler, S. André, G. Schön, U. Hübner, H. G. Meyer, E. Llichev, A. V. Ustinov, *Nat. Commun.* **2014**, *5*, 5146.
[20] P. K. Jha, M. Mrejen, J. Kim, C. Wu, Y. Wang, Y. V. Rostovtsev, X. Zhang, *Phys. Rev. Lett.* **2016**, *116*, 165502.
[21] N. Yu, F. Capasso, *Nat. Mater.* **2014**, *13*, 139.
[22] A. V. Kildishev, A. Boltasseva, V. M. Shalaev, *Science* **2013**, *339*, 1232009.
[23] M. Khorasaninejad, W. T. Chen, R. C. Devlin, J. Oh, A. Y. Zhu, F. Capasso, *Science* **2016**, *347*, 1190.
[24] C. D. Giovampaola, N. Engheta, *Nat. Mater.* **2014**, *13*, 1115.
[25] N. I. Zheludev, Y. S. Kivshar, *Nat. Mater.* **2012**, *11*, 917.
[26] T. Ergin, N. Stenger, P. Brenner, J. B. Pendry, M. Wegener, *Science* **2009**, *328*, 337.
[27] R. Liu, C. Ji, J. J. Mock, J. Y. Chin, T. J. Cui, D. R. Smith, *Science* **2009**, *323*, 366.
[28] A. Silva, F. Monticone, G. Castaldi, V. Galdi, A. Alù, N. Engheta, *Science* **2014**, *343*, 160.
[29] A. Pors, M. G. Nielsen, S. I. Bozhevolnyi, *Nano Lett.* **2014**, *15*, 791.

 

[30] Y. Hwang, T. J. Davis, *Appl. Phys. Lett.* **2016**, *109*, 181101.
[31] A. Youssefi, F. Zangeneh-Nejad, S. Abdollahramezani, A. Khavasi, *Opt. Lett.* **2016**, *41*, 3467.
[32] W. Zhang, C. Qu, X. Zhang, *J. Opt.* **2016**, *18*, 075102.
[33] T. Zhu, Y. Zhou, Y. Lou, H. Ye, M. Qiu, Z. Ruan, S. Fan,